ORIGINAL ARTICLE

A new halothermal time model describes seed germination responses to salinity across both sub- and supra-optimal temperatures

Esmaeil Bakhshandeh[1] · Kent J. Bradford[2] · Hemmatollah Pirdashti[1] · Fatemeh Vahabinia[1] · Raoudha Abdellaoui[3]

Abstract

We quantified the seed germination responses of chicory (*Cichorium intybus* L.; Asteraceae) to heat, water and salt stresses using hydrothermal time (HTT) and halothermal time (HaloTT) models. We extended the HaloTT model based on NaCl concentration to include supra-optimal temperatures. The HTT and HaloTT models enabled quantitative comparison of the effects of reduced water potentials and increased salinity on germination. Below 30 °C, the median threshold water potential permitting germination estimated by the HTT model (-0.83 MPa) was higher than that estimated by the HaloTT model (-1.30 MPa, after converting the median threshold NaCl concentration to osmotic potential). Ion uptake into seeds imbibed in salt solutions accounted for an average osmotic adjustment of 36% in the presence of salt stress compared to seeds imbibed in polyethylene glycol solutions. These thresholds became more positive above 30 °C with a common median ceiling temperature of 43 °C. The HaloTT models developed here accurately described germination responses to NaCl concentrations across all temperatures and incorporated both water potential and osmotic adjustment effects. With respect to seed germination, chicory could be considered as a moderately water stress tolerant species and highly tolerant to salt stress.

Abbreviations

Cl^-	Chloride ion
GP	Germination percentage
GR	Germination rate, or $1/t_g$
HaloTT	Halothermal time model
HTT	Hydrothermal time model
k_T	The slope of the relationship between $\psi_b(50)$ and/or $NaCl_b(50)$ and T above T_o

M	Molar
MPa	Megapascal
Na^+	Sodium ion
NaCl	NaCl concentration (M)
$NaCl_b(50)$	The base NaCl of the 50th percentile
$NaCl_b$	Median base NaCl concentration
OAV	Osmotic adjustment value
SG	Seed germination
SMC	Seed moisture content
T	Temperature
T_b	Minimum temperature (base temperature)
T_c	Maximum temperature (ceiling temperature)
T_d	The temperature at which $\psi_b(50)$ and/or $NaCl_b(50)$ trend begins to change
t_g	The time required for fraction or percentage (g) of seeds to germinate
T_o	Optimum temperature
θ_H	Hydrotime constant
θ_{Halo}	Halotime constant
σ_{NaClb}	Standard deviation of $NaCl_b$ within the seed population
$\sigma\psi_b$	Standard deviation of ψ_b within the seed population

Communicated by S. Renault.

✉ Esmaeil Bakhshandeh
bakhshandehesmail@gmail.com; e.bakhshandeh@sanru.ac.ir

1 Genetics and Agricultural Biotechnology Institute of Tabarestan and Sari Agricultural Sciences and Natural Resources University, Km 9 Farah Abad Road, P.O. Box: 578, Sari City, Mazandaran Province Postal code: 4818168984, Iran

2 Department of Plant Sciences, Seed Biotechnology Center, University of California, Davis, CA 95616, USA

3 Laboratoire des Ecosystèmes Pastoraux et Valorisation des Plantes Spontanées et des Micro-organismes Associés, Institut des Régions Arides, Université de Gabes 4119 Médenine, Gabès, Tunisia

ψ Water potential

$\psi_b(50)$ The base ψ of the 50th percentile

ψ_b Base water potential

Introduction

Seed germination (SG) is a complex physiological process that is affected by abiotic stresses, including temperature (T), water stress, and salinity, and by other physical and biological factors (Bradford 2002; Bakhshandeh et al. 2020; Vahabinia et al. 2019). T is a critical factor affecting both the germination percentage (GP) and the germination rate (GR, or $1/t_g$) (Ghaderi-Far et al. 2010; Bewley et al. 2013). During the germination phase of the plant life cycle, there exists a T below which germination is prevented, called the base temperature (T_b), an optimum temperature (T_o, single and/or range of Ts) at which germination is most rapid, and a T above which germination does not occur, called the ceiling temperature (T_c) (Bakhshandeh et al. 2013). These so-called cardinal Ts vary depending on species and environmental conditions under which they were produced (Hatfield and Prueger 2015). GR usually increases linearly with T between T_b and T_o, and declines linearly and/or curvilinearly at $Ts > T_o$ (Bradford 2002; Rowse and Finch-Savage 2003; Mesgaran et al. 2017; Abdellaoui et al. 2019). Water availability is an important factor affecting SG and failure or success of plant establishment. Commonly, GP and GR increase with water availability and decrease at more negative water potential (ψ) (Mesgaran et al. 2013; Atashi et al. 2015). Salinity may limit SG through both osmotic and ion-specific effects (Zhang et al. 2010; Llanes et al. 2016). Dissolved salts decrease the ψ of saline solutions, with a 1 M solution of NaCl having a ψ of approximately -4.4 MPa at 25 °C (Nobel 1983). In addition, accumulations of inorganic ions (e.g., sodium [Na^+] and chloride [Cl^-]) and compatible organic solutes (e.g., amino acids, proline, etc.) result in osmotic adjustment, or a reduction of ψ inside the seed cells, that can enable SG to occur at lower water potentials (Parihar et al. 2015; Seal et al. 2018). These factors, T, ψ and salinity, influence SG alone and/or in combination, and are relevant to crop production and to ecological distributions of species (Baskin and Baskin 2014).

The hydrotime model developed by Gummerson (1986) and Bradford (1990) has been used to quantify the influence of ψ on germination at a given T. According to the model, the time to germination is inversely proportional to the difference between the ψ of the seed environment and the physiological ψ threshold for radicle emergence (base ψ or ψ_b), which varies among seeds in the population. The ψ_b values for various germination percentiles ($\psi_b(g)$) usually exhibit a normal distribution within seed populations (Dahal and Bradford 1994; Bradford and Still

2004; Bakhshandeh and Gholamhosseini 2018), although other distributions, such as Gumbel, Weibull, Log-Normal, Logistic, Log-logistic, Inverse Normal and Gamma, have been applied to specific seed populations or mixtures of populations (Mesgaran et al. 2013; Atashi et al. 2015; Moltchanova et al. 2020).

Gummerson (1986) also proposed a hydrothermal time (HTT) model of SG stating that at $Ts \leq T_o$ (i.e., between T_b and T_o) and at any constant ψ, the time to germination (t_g) of any germination percentile of a seed population is a function of the degree to which T and ψ exceed their respective base values, T_b and ψ_b, at which germination is inhibited (Gummerson 1986; Dahal and Bradford 1994; Bradford 1995). In this model, Gummerson (1986) assumed that θ_{HT} and T_b are constant and equal among seeds and only $\psi_b(g)$ varies in the seed population. However, this model does not predict the inhibition of SG (both GR and GP) at $Ts > T_o$ (i.e., between T_o and T_c). Consequently, Alvarado and Bradford (2002) suggested another model in which the relationship between GR vs. T will be negatively linear at $Ts > T_o$ with a common T_o for all germination percentiles but differing T_c values in the population. This decline in GR and GP was due to a linear increase in $\psi_b(g)$ as T increased above T_o, and a constant value (i.e., k_T) was defined as the increase in $\psi_b(50)$ per degree as T increased above T_o. This modeling approach successfully predicted SG in many crops, such as potato (*Solanum tuberosum* L.) (Alvarado and Bradford 2002), watermelon (*Citrullus vulgaris*) (Bakhshandeh et al. 2015), sesame (*Sesamum indicum* L.) (Bakhshandeh et al. 2017) and eruca (*Eruca sativa*) (Bakhshandeh et al. 2019).

However, for some other crops such as wild barley (*Hordeum spontaneum* Thell.) and little canarygrass (*Phalaris minor* L.) (Mesgaran et al. 2017) and *Retama reatam* (Abdellaoui et al. 2019), the relationship between GR and T did not transition sharply from increasing to decreasing at T_o. Rowse and Finch-Savage (2003) showed also that a T lower than T_o should be defined (T_d) at which $\psi_b(50)$ starts to change, i.e., $[\psi - \psi_b(50) + k_T(T - T_d)]$, resulting in a curvilinear peak in GR around and above T_o (e.g., Bakhshandeh and Gholamhosseini 2019).

Seal et al. (2018) used the same methodology to quantify the SG characteristics of the halophyte *Suaeda maritima* under different NaCl concentrations at sub-optimal Ts. They developed a halothermal time (HaloTT) model that utilized log NaCl to replace water potential in the HTT model. That is, the germination behavior at sub-optimal Ts was governed by the salt concentration threshold distribution ($NaCl_b(g)$) relative to the NaCl of the environment. In the current work, we employ the HaloTT model and extend it to describe SG in response to T across all Ts at any constant NaCl concentration. To our knowledge, no HaloTT model to quantify SG responses at supra-optimal Ts has been proposed as yet, thus, our study is the first report in this case.

Chicory (*Cichorium intybus* L.; Asteraceae) is a perennial herb, native to Europe, Africa, America and many parts of Asia, including Iran (Jouad et al. 2001; Benítez et al. 2010; Guarrera and Savo 2016). The medicinal effects of chicory are well documented (Abbas et al. 2015; Sampaio et al. 2009; Yoo et al. 2011). Furthermore, this plant copes with different soil types and abiotic and biotic stresses and can be used as food and feed. Based on its broad tolerance to environmental conditions, we have investigated the SG responses of chicory to combinations of T, ψ and salinity using the models described above. The aims of this study were: (1) to study the effects of heat, water and salt stresses on SG characteristics of chicory; (2) to estimate the cardinal Ts for germination using the HTT and HaloTT models; (3) to measure the uptake of salt ions into chicory seeds in response to salinity; and (4) to calculate the amount of osmotic adjustment attributable to NaCl uptake into the seeds when imbibed in salt solutions.

Materials and methods

Seed collection and treatments

Chicory seeds were provided from Mazandaran province, Iran, in 2017. They were maintained in the dark at 5 °C for 3 months. The seed viability [assessed according to ISTA (2018)] was > 98% under optimal conditions at the beginning of the experiments. The treatments were seven constant Ts (10, 15, 20, 25, 30, 35 and 40 °C), four levels of ψ (− 0.3, − 0.6, − 0.9 and − 1.5 MPa) and four levels of salinity (0.075, 0.150, 0.225 and 0.300 M). For the control we used distilled water in all experiments. Polyethylene glycol (PEG8000, Scharlau, Spain) was applied to make solutions having different ψs (and corrected for Ts) based on Michel and Radcliffe (1995) method. An osmometer (Model 5520: Wescor Inc., USA) was used initially and also every two days during the experiments to re-check the ψs for each T. Sodium chloride (NaCl) was applied to prepare different levels of salt stress that are mentioned above. The NaCl concentration (M) at each T was converted to water potential (ψ, MPa) according to the Van't Hoff relation (Van't Hoff 1887), and confirmed using the osmometer as well.

Seed germination tests

Fifty seeds for each of four replicates per treatment were placed on two sheets of Whatman No. 1 filter paper within 8 cm Petri dishes with six mL of the test solutions, supported by 0.1% Thiram. An incubator with ± 0.5 °C precision was used and the Petri dishes were randomly placed within in the dark, except during recording times. The Petri dishes were put into a plastic bag to avoid water

evaporation. Seeds were counted several times daily, depending on the T, ψ and salt stress in all experiments. The seeds at least 2 mm long of radicle were considered as germinated seeds. At each counting time, germinated seeds were removed to avoid an error. The experiments were ended when no additional seeds germinated for three consecutive days.

Hydrotime and halotime models

A repeated probit regression analysis as followed by Bradford (1990) were used to analyses and determine the model parameters. GR_{50} (h^{-1}) was calculated by interpolation by curves fit to the time course data according to:

$$GR_{50} = 1/t_{50}, \tag{1}$$

where GR_{50} is the GR for the 50th percentile of germination (h^{-1}) and t_{50} is the time to reach 50% germination.

To quantify the germination time courses data in the osmotic solutions at 10, 15, 20, 25, 30, 35 and 40 °C, the hydrotime model was used. This model is expressed as (Gummerson 1986):

$$\theta_H = \left(\psi - \psi_b(g)\right)t_g, \tag{2}$$

where θ_H is the hydrotime constant (MPa h or MPa d); ψ is the actual water potential of the medium (MPa); $\psi_b(g)$ is the base value of ψ inhibiting radicle emergence of percentage g (MPa); and t_g is the actual time to germination of percentage g. Thus, the $\psi_b(50)$ is the base water potential for the median or 50th percentile SG fraction.

A similar method was used to determine the parameters of halotime model by substituting the NaCl for ψ, the $NaCl_b(g)$ for $\psi_b(g)$ and the θ_{Halo} for θ_H. For each salt treatment at 10, 15, 20, 25, 30, 35 and 40 °C, the halotime model can be written as (Seal et al. 2018):

$$\theta_{Halo} = \left(NaCl_b(g) - NaCl\right)t_g, \tag{3}$$

where θ_{Halo} is the halotime constant (M h or M d); $NaCl_b(g)$ is the base value of NaCl inhibiting radicle emergence of percentage g (M); NaCl is concentration of the imbibition medium (M); and t_g is the actual time to germination percentage g (h or d). Thus, the $NaCl_b(50)$ is the median base NaCl concentration for the 50th percentile SG fraction. We note that the original equation in Seal et al. (2018) would result in negative values for θ_{Halo} since the term used there ($NaCl - NaCl_b(g)$) [or $NaCl_{max\ g}$ as defined in Seal et al. (2018)] will be a negative number, as the magnitude of NaCl is smaller than $NaCl_b(50)$ at any NaCl permitting germination. We have reversed the order of $NaCl_b(g)$ and NaCl in Eq. 3 to give positive values of θ_{HaloTT}.

Hydrothermal time and halothermal time models

At $Ts \leq T_o$, the HTT model is expressed as (Gummerson 1986):

$$\theta_{\text{HTT}} = (\psi - \psi_b(g))(T - T_b)t_g, \tag{4}$$

or

$$\text{Probit (g)} = [\psi - (\theta_{\text{HTT}}/(T - T_b)t_g) - \psi_b(50)]/\sigma_{\psi b}. \tag{5}$$

At $Ts > T_o$, the model should be modified to (Alvarado and Bradford 2002):

$$\theta_{\text{HTT}} = [\psi - (\psi_b(g) + k_T(T - T_d))](T - T_b)t_g, \tag{6}$$

or

$$\text{Probit (g)} = \{[(\psi - k_T(T - T_d)) - \theta_{\text{HT}}/((T - T_b)t_g)] - \psi_b(50)\}/\sigma_{\psi b}, \tag{7}$$

where T_d represents the T at which GR begins to be affected by warm Ts, which can be lower than T_o (Rowse and Finch-Savage 2003).

For the HaloTT model, the model proposed by Seal et al. (2018) (with correction as above) at $Ts \leq T_o$ was used:

$$\theta_{\text{HaloTT}} = (\text{NaCl}_b(g) - \text{NaCl})(T - T_b)t_g, \tag{8}$$

or

$$\text{Probit (g)} = [\text{NaCl} + (\theta_{\text{HaloTT}}/(T - T_b)t_g) - \text{NaCl}_b(50)]/\sigma_{\text{NaClb}}, \tag{9}$$

where θ_{HaloTT} is the HaloTT constant (M °C h or M °C d) and σ_{NaClb} is the standard deviation of the $\text{NaCl}_b(g)$ distribution.

To our knowledge, no HaloTT model to quantify SG responses at $Ts > T_o$ has been proposed as yet. Thus, we developed the model below as the first report:

$$\theta_{\text{HaloTT}} = [\text{NaCl}_b(50) - (\text{NaCl} + k_T(T - T_d))](T - T_b)t_g, \tag{10}$$

or

$$\text{Probit (g)} = [(\text{NaCl} + k_T(T - T_d)) + (\theta_{\text{Halo}}/(T - T_b)t_g) - \text{NaCl}_b(50)]/\sigma_{\text{NaClb}}. \tag{11}$$

Thus, SG response can be quantified at all Ts and ψs by the HTT models (Eqs. 4–7) and at all Ts and NaCls using the HaloTT models (Eqs. 8–11).

Seed moisture contents

Three replicates of 1 g chicory seeds were sown on two sheets of Whatman No. 1 filter paper in 8 cm Petri dishes containing 6 mL of water, 0.075, 0.150, 0.225 and 0.300 M NaCl at 10, 15, 20, 25, 30, 35 and 40 °C. Immediately prior to the initiation of germination (estimated from the cumulative GP vs. time curve, Fig. 2), seeds were rinsed several times with distilled water and blotted with filter paper to remove any solution from the testa. The seeds weighted, then dried in an oven at 103 °C for 17 h (ISTA 2018) and seed moisture content (SMC) was expressed on a dry weight basis.

Seed Na⁺ and Cl⁻ concentrations and estimated osmolality

A flame photometric method as described by Estefan et al. (2013) was used to measure Na^+ concentration in the chicory seeds obtained from the experiment described above (seed moisture contents section). Dried chicory seeds (103 °C for 17 h) were powdered by a mill and 0.5 g for each replicate was oxidized at 550 °C for 5 h and 2 N hydrochloric acid was used to digest the dry residue. Na^+ was analyzed using a flame photometric instrument (model PFP7, Jenway, UK) and standard curves were constructed using 1000 ppm Na flame photometry standard solution (Product No: 025021, Jenway, UK) for quantification. To determine chloride (Cl^-) concentration in the seeds, 0.2 g of dry powdered seeds for each replicate was placed in 20 mL of distilled water at > 90 °C for 1 h, then the amount of Cl^- was measured by AgNO_3 (Mohrs's titration) method (Estefan et al. 2013). The summed concentrations of Na^+ and Cl^- (mmol kg DW^{-1}) were divided by the seed water content (kg H_2O kg DW^{-1}) at the time of sampling to estimate the total osmolality (mmol/kg H_2O) contributed by these ions, making the simplifying assumption that all of the water in the seed was symplastic. We then used the Van't Hoff relation to convert the osmolality of salt ions in the seeds to ψ (MPa).

Statistical analyses

All statistical analyses were performed using the Statistical Analysis System ver. 9.4 (SAS Institute 2015), Excel and

Sigma Plot ver. 11 software (Systat Software Inc., San Jose CA, USA, www.systatsoftware.com). A two-way ANOVA with the least significant difference test (LSD) at 0.05 probability level was used to analyze the effects of T, ψ, salinity and their interactions on SG, seed Na^+ and Cl^- concentrations and SMC.

Results

Effects of water potential, temperature and salinity on GP and GR

Water potential, NaCl and their interactions significantly affected GP and GR_{50} ($p > 0.001$) (Table 1). Supra-optimal T reduced GP (in water) while ψ and/or NaCl reduced GP at both lower and higher T. Both GP and GR_{50} decreased with decreasing ψ (Fig. 1) and with increasing NaCl in the medium at each tested T (Fig. 2). The relationship between GR_{50} and T was linear at $T < 30$ °C (sub-optimal Ts) under both conditions and shared a common T_b (Fig. 3). In general,

GP and GR_{50} were more sensitive to changes in ψ and/or NaCl than to changes in T (Figs. 1, 2).

Hydrotime and halotime models

The hydrotime model successfully described germination data across all ψs at each T, with $R^2 > 0.88$ (Table 2; Fig. 1). The θ_H values declined with increasing T from 62.9 MPa h at 10 °C to 9.0 MPa h at 30 °C and was fixed to a constant value of 9.0 MPa h at $Ts > 30$ °C (i.e., $Ts > T_o$) because this optimized the model (Table 2; Fig. 3a). The inverse of θ_H values ($1/\theta_H$) was linear below T_o (and extrapolated to $T_b = 4.8$ °C, on the x axis) (Fig. 3a). The $\psi_b(50)$ remained approximately constant at sub-optimal Ts (i.e., ≤ 30 °C), ranging from -0.813 to -0.839 MPa, then increased linearly to -0.573 and -0.210 MPa at 35 and 40 °C, respectively, and intersected 0 MPa at 43 °C (i.e., $T_c(50)$) (Table 2; Fig. 3b) The $\psi_b(50)$ values increased with increasing T above T_o with a k_T (slope) value of 0.066 MPa °C^{-1} (Table 2; Fig. 3b).

Table 1 Analysis of variance (mean squares) and means comparison for germination percentage (GP) and median germination rate (GR_{50}) of chicory as influenced by temperature (T), water potential (ψ) and salinity (NaCl)

Source of variation	Water stress			Salt stress			
	df	GP	GR_{50}		df	GP	GR_{50}
T	6	1.342***	0.0021***	T	6	0.904***	0.00424***
Error 1	21	0.020	0.00002	Error 1	14	0.037	0.000024
ψ	3	5.918***	0.0125***	NaCl	4	3.519***	0.01306***
$T \times \psi$	18	0.204***	0.00050***	$T \times$ NaCl	24	0.089***	0.00006***
Error 2	63	0.018	0.000012	Error 2	56	0.028	0.000809
Coefficient of variation (%)		12.0	16.5			10.5	14.4
Means comparison[†]	T (°C)	GP (%)	GR_{50} (h^{-1})	T (°C)	GP (%)	GR_{50} (h^{-1})	
T (°C)	10	56.6c	0.0088e	10	84.4ab	0.0137e	
	15	73.6a	0.0164d	15	83.5ab	0.0186d	
	20	78.0a	0.0282b	20	88.0a	0.0354c	
	25	76.4a	0.0375a	25	82.2ab	0.0441b	
	30	63.5b	0.0386a	30	74.6b	0.0709a	
	35	52.5d	0.0375a	35	55.3c	0.0429b	
	40	17.6e	0.0219c	40	46.2d	0.0227d	
	MPa	GP (%)	GR_{50} (h^{-1})	M	GP (%)	GR_{50} (h^{-1})	
MPa or M	0	86.8a	0.0545a	0	95.3a	0.0731a	
	-0.3	82.5a	0.0325b	0.075	90.4b	0.0457b	
	-0.6	53.4b	0.0145c	0.150	76.3c	0.0282c	
	-0.9	12.2c	0.0069d	0.225	58.8d	0.0154d	
	-1.5	–	–	0.300	32.2e	0.0056e	

df = degrees of freedom. The seeds were unable to germinate at -1.5 MPa. The number of points in water stress is $n = 112$ ($T = 7$, $\psi = 4$ and replications = 4) and in salinity is $n = 105$ ($T = 7$, NaCl (M) = 5 and replications = 3)

*** highly significant at 0.001 probability level

[†]Means with the same letter are not significantly different based on the Duncan's multiple range test
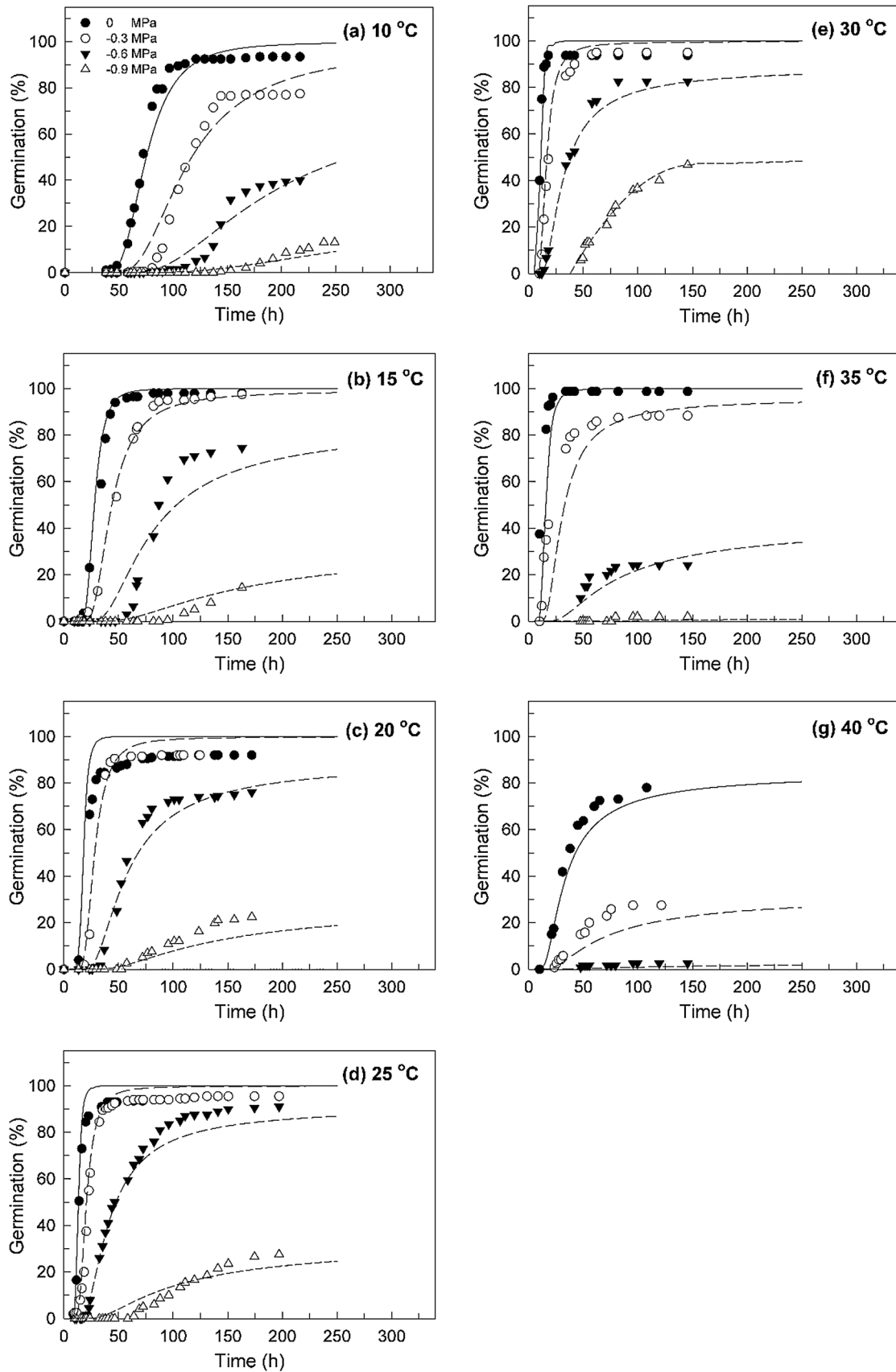
Fig. 1 Chicory seed germination at different temperatures under various water potentials
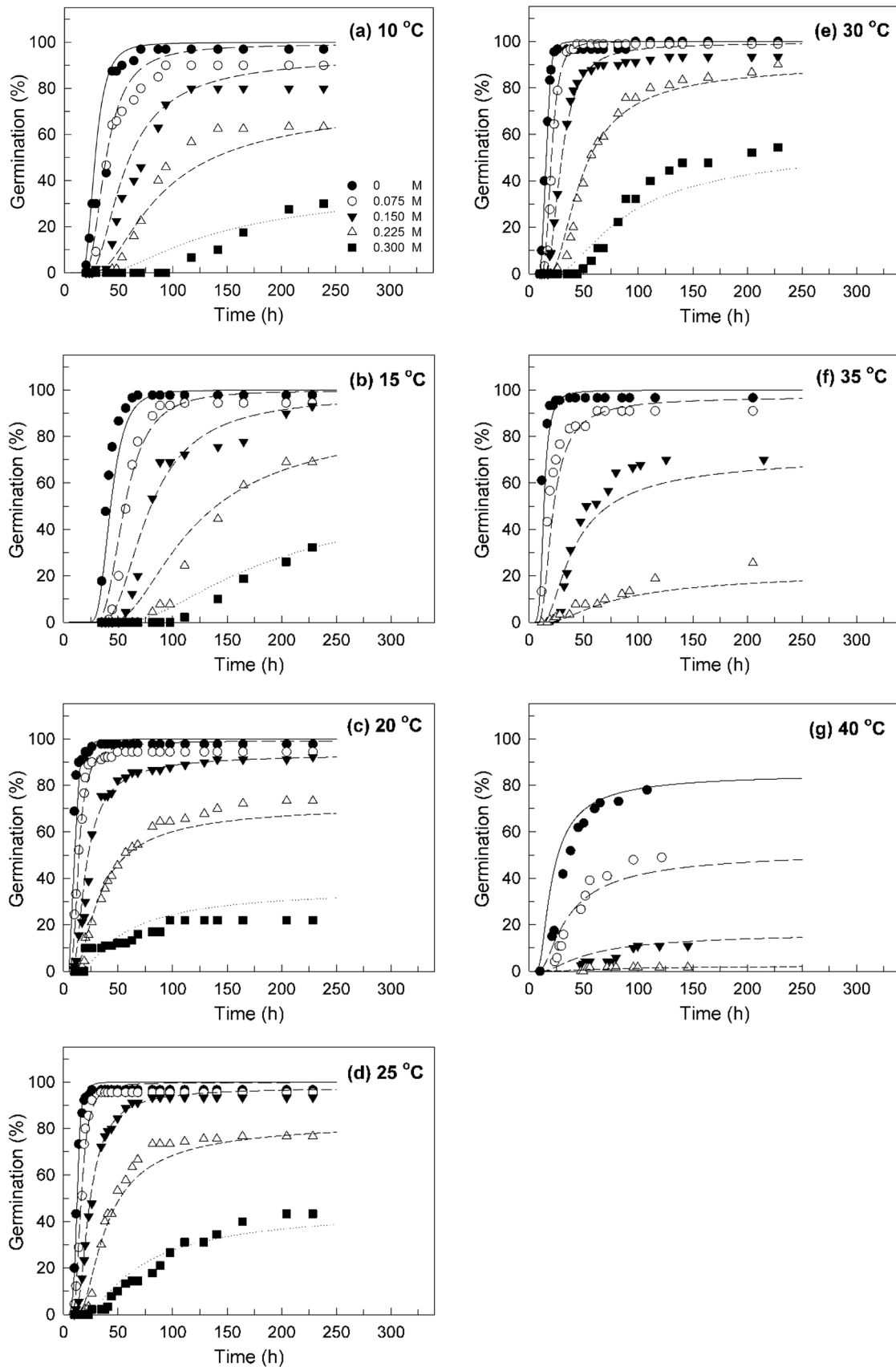
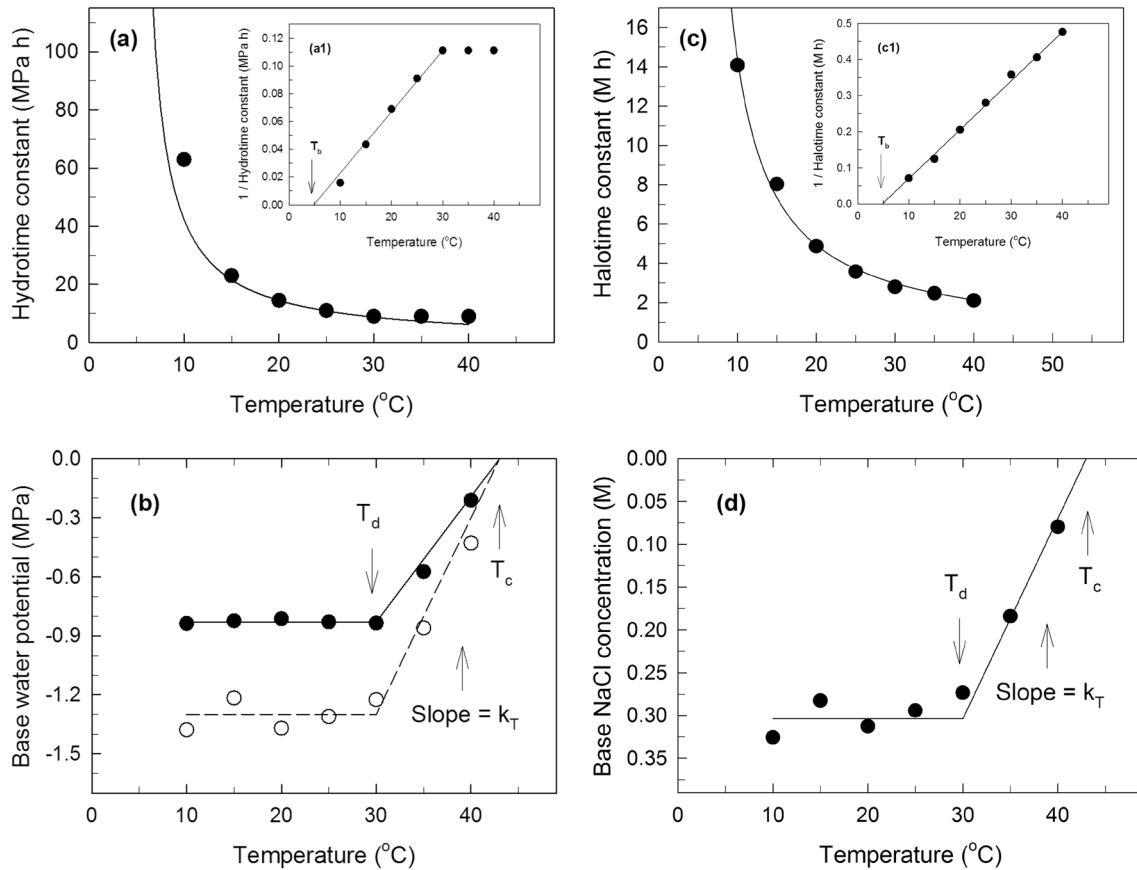**Fig. 2** Chicory seed germination at different temperatures under various concentrations of NaCl

Fig. 3 Hydrotime constant (θ_H, **a**), base water potential ($\psi_b(50)$, closed circles and solid line) and base $NaCl_b(50)$ after converting to MPa by van't Hoff equation (open circles and dashed line; **b**), halotime constant (θ_{Halo}, **c**) and base NaCl concentration ($NaCl_b(50)$, **d**) as a function of temperature (T) for chicory seeds. In **b** and **d**, the predicted lines are for the 50th percentile intercepts $\psi_b(50) = 0$ MPa and

$NaCl_b(50) = 0$ MPa at T_c (43 °C), respectively. Inset a1: the inverse of θ_H vs. T, which will be linear below T_o (and extrapolates to T_b at the intercept on the x axis) and then is constant at $T > T_o$, as this maximized the fitting of the model. Inset c1: the inverse of θ_{Halo} vs. T, which continues increasing linearly up to 40 °C

We used the same method to estimate the parameters of the halotime model at each T, with R^2 ranging from 0.82 to 0.97 (Table 2; Fig. 2). The θ_{Halo} values non-linearly decreased with increasing T from 14.1 M h at 10 °C to 2.1 M h at 40 °C (Table 2; Fig. 3c). The inverse of θ_{Halo} values ($1/\theta_{Halo}$) were linear with T up to 40 °C and intercepted the x axis at $T_b = 4.8$ °C (Fig. 3c). The $NaCl_b(50)$ for chicory seeds remained approximately constant at suboptimal Ts (i.e., < 30 °C), ranging from 0.294 to 0.326 M, then decreased linearly ($k_T = 0.024$ M °C^{-1}) with increasing T above T_o until it intersected 0 M at 43 °C (i.e., $T_c(50)$) (Table 2; Fig. 3d). That is, the NaCl required to prevent germination decreased by 0.024 M per degree above T_o (Table 2; Fig. 3d).

The median GR_{50} ($1/t_{50}$) across Ts at different ψs increased linearly at $Ts \leq T_d$, the T at which $\psi_b(50)$ begins to change (which is equal to T_o in this case), and then decreased non-linearly at Ts above T_o until T_c (Fig. 4a). The maximum GR_{50} (0.0973 h^{-1}) was observed at T_o when $\psi = 0$ MPa

and then decreased linearly as ψ increased, reaching zero at -0.83 MPa with a rate of decrease of 0.111 h^{-1} per MPa with decreasing ψ (Fig. 4b). The common intercept at $T_b = 4.8$ °C (Table 3; Fig. 4a), indicates that base temperature was not affected by ψ. In contrast, the linear decrease in $T_c(50)$ values predicted by the HTT model as T increases above T_o (i.e., 30 °C) is illustrated in Fig. 4c.

The relationship of GR_{50} with T at different NaCl concentrations showed a similar pattern as was observed for ψ (Fig. 4d). GR_{50} reached its maximum (0.0979 h^{-1}) at T_o when NaCl = 0 M and then decreased linearly as NaCl concentration increased, reaching zero at 0.304 M (-1.37 MPa, after converting to ψ) with a rate of decrease of 0.32 h^{-1} per M of increase in NaCl (Fig. 4e). The linear decrease in $T_c(50)$ values predicted by the HaloTT model relative to the control (NaCl = 0 M) as NaCl increased between 43 and 30 °C is also shown (Fig. 4f).

When the initial salinity levels tested were converted into ψ values (using the Van't Hoff equation), the calculated

Table 2 The hydrotime (Eq. 2) and halotime (Eq. 3) models parameters for describing chicory seed germination under different Ts and ψs and Ts and NaCl concentrations, respectively. R^2 is the coefficient of determination

Model type	T (°C)	θ_H (MPa h)	$\psi_b(50)$ (MPa)	$\sigma_{\psi b}$ (MPa)		R^2
Hydrotime	10	62.9	− 0.837	0.236		0.92
	15	23.0	− 0.823	0.205		0.88
	20	14.5	− 0.813	0.164		0.97
	25	11.0	− 0.830	0.166		0.95
	30	9.00	− 0.839	0.191		0.94
	35	9.00	− 0.573	0.152		0.89
	40	9.00	− 0.210	0.202		0.96
	T (°C)	θ_{Halo} (M h)	$NaCl_b(50)$ (M)	σ_{NaClb} (M)		R^2
Halotime	10	14.1	0.325	0.077		0.82
	15	8.03	0.283	0.078		0.89
	20	4.87	0.312	0.062		0.94
	25	3.57	0.294	0.069		0.97
	30	2.79	0.273	0.079		0.95
	35	2.46	0.184	0.055		0.97
	40	2.10	0.080	0.074		0.94
	T (°C)	θ_H (MPa h)	$\psi_b(50)$ (MPa)	$\sigma_{\psi b}$ (MPa)	R^2	OAV (%)
Hydrotime after converting NaCl to ψ[†]	10	59.5	− 1.37	0.283	0.82	39.2
	15	37.1	− 1.21	0.337	0.89	32.3
	20	21.3	− 1.36	0.274	0.94	40.6
	25	15.9	− 1.31	0.310	0.97	36.7
	30	12.5	− 1.22	0.338	0.97	31.4
	35	12.5	− 0.96	0.277	0.93	40.3
	40	12.5	− 0.45	0.295	0.97	53.1

The value of θ_H value (9.0 MPa h) was derived to be constant at $T > T_o$, for better fitting of the model

Osmotic adjustment value (%, OAV) was calculated by the following model [OAV = (1 − (estimated $\psi_b(50)$ value using hydrotime model/estimated $\psi_b(50)$ value using halotime model after converting NaCl to ψ)) × 100]

[†]The NaCl concentrations (M) values were converted to water potentials (MPa) using van't Hoff equation

$\psi_b(50)$ values were much lower (more negative) in comparison with PEG data (Table 2; Fig. 3b). For example, at 40 °C, the estimated $\psi_b(50)$ was − 0.21 MPa in PEG but was − 0.45 in NaCl. This could be due to Na$^+$ and Cl$^-$ ions entering into seed cells, lowering their osmotic potential and increasing embryonic turgor, enabling the seeds to germinate at lower ψs. The relative osmotic adjustment of the chicory seeds imbibed in NaCl was calculated as [(1 − (estimated $\psi_b(50)$ using hydrotime model/estimated $\psi_b(50)$ using the halotime model after converting NaCl to ψ)) × 100]. This Osmotic Adjustment Value was relatively constant (32 to 40%) at $T < T_o$, then increased above T_o as the value of $\psi_b(50)$ became less negative (Tables 2, 3).

The $\sigma_{\psi b}$ and σ_{NaClb} values varied little across Ts (Table 2), indicating that to the variation of ψ and NaCl thresholds among individual seeds did not change across the range of temperatures tested.

Hydrothermal time model, halothermal time model and cardinal temperatures

To quantify the response of chicory SG to across all Ts under different ψ and NaCl, HTT (Eqs. 4, 7) and HaloTT (Eqs. 8, 11) models were applied to the respective data. The HTT model described the SG data of chicory well, with R^2 of 0.86 (Table 3; Fig. 5a). The estimated parameters were 220 MPa °C h for θ_{HTT}, − 0.83 MPa for $\psi_b(50)$, 0.211 MPa for $\sigma_{\psi b}$ and 0.066 MPa °C^{-1} for k_T (Table 3).

The HaloTT model fit the data for chicory SG in NaCl with a high R^2 value (0.83) (Table 3; Fig. 5b) and an estimated θ_{HaloTT} value of 74.9 M °C h (Table 3). The osmotic adjustment value was 36% when the $\psi_b(50)$ value estimated by the HTT (− 0.83 MPa) was compared to the $\psi_b(50)$ value estimated by the HaloTT (− 1.30 MPa) (Table 3).
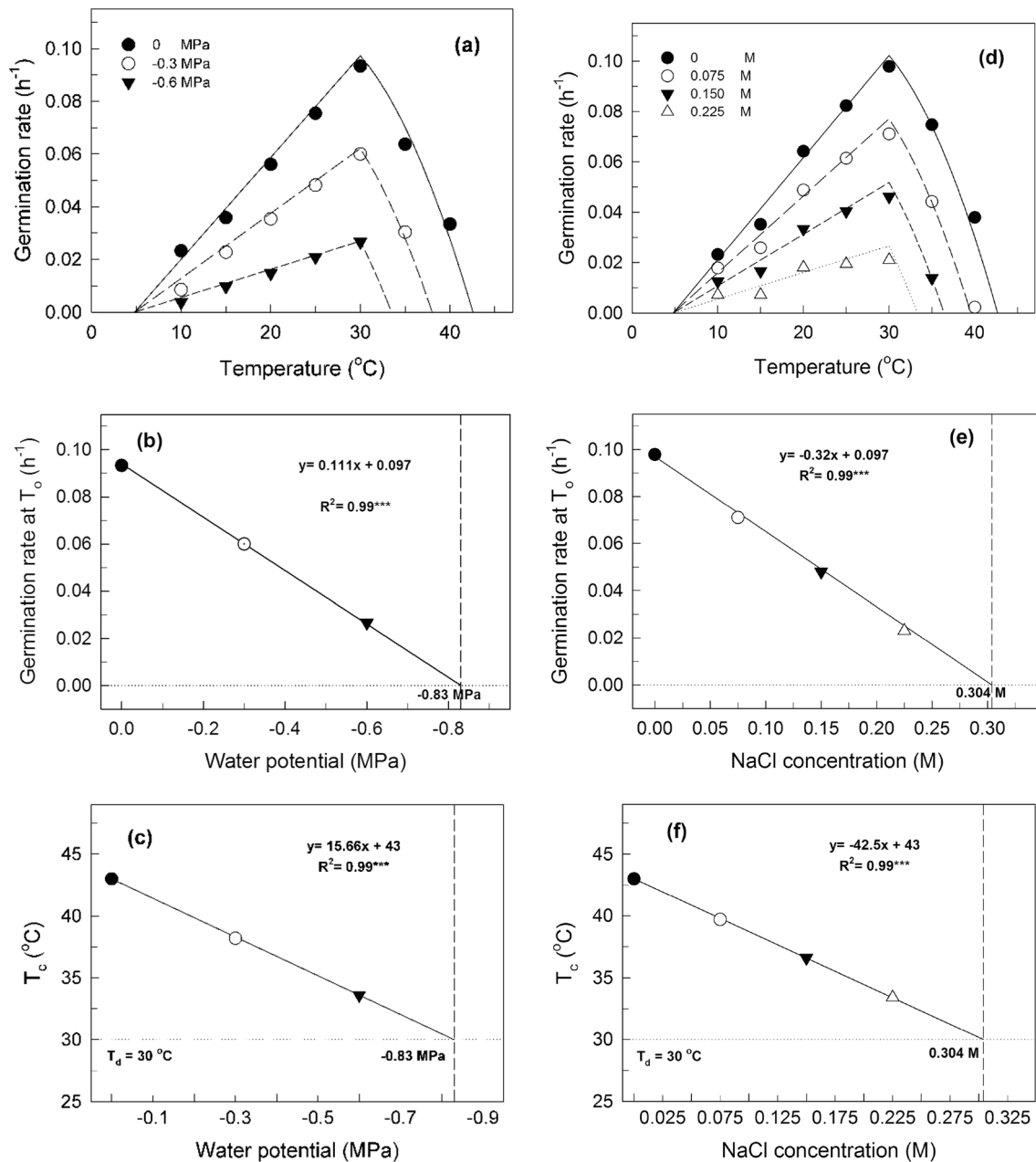
Fig. 4 The effect of temperature (T) and water potential (MPa) (**a**) and T and NaCl concentration (M) (**d**) on the median germination rates ($= 1/t_{50}$) of chicory seeds. The symbols represent the actual data and the lines drawn through these points are based upon the parameters of the hydrothermal time and halothermal time models (Table 3). The effects of ψ and of NaCl on GR_{50} at T_o (**b**, **e**, respectively) intersect the calculated $\psi_b(50)$ and $NaCl_b(50)$ values at $GR_{50} = 0$ or $T_c = T_d = T_o$ and the linear relationships were highly significant ($P < 0.0001$). The $T_c(50)$ values predicted by the hydrothermal and halothermal models at each ψ or NaCl also are shown (**c**, **f**, respectively), and therefore fall exactly on the modeled lines

To determine the cardinal Ts for chicory, GR_{50} vs. T was plotted in both conditions. The relationships between GR_{50} and $Ts \leq T_o$ were linear at all ψs and all NaCls and were limited to a single T_b of 4.8 °C (Fig. 4a, d). GR_{50} reached its maximum at T_o (30 °C) in both conditions (water and/or salt stresses) and also was not influenced by ψ and NaCl. Similarly, $T_c(50)$ was 43 °C based on both the HTT and HaloTT models (Fig. 3b, d).

Seed moisture content and osmotic adjustment to salt

SMC was measured just prior to radicle emergence at different Ts and NaCls (Fig. 6a). At 10 °C, SMC was unchanged under salt stress relative to control (NaCl = 0 M). However, SMC decreased with increasing T from 15 to 30 °C under

Table 3 Estimated parameter values using the hydrothermal time (HTT; Eqs. 4, 7) and halothermal time (HaloTT; Eqs. 8, 11) models for describing seed germination of chicory at seven constant Ts (10, 15, 20, 25, 30, 35 and 40 °C) at each of four different ψs (0, −0.3, −0.6 and −0.9 MPa) and/or five different NaCls (0, 0.075, 0.150, 0.225 and 0.300 M)

HTT parameters		HaloTT parameters		HaloTT parameters after converting NaCl to ψ values	
$\psi_b(50)$ (MPa)	−0.83	$NaCl_b(50)$ (M)	0.304	$\psi_b(50)$ (MPa)	−1.30
$\sigma_{\psi b}$ (MPa)	0.211	σ_{NaClb} (M)	0.075	$\sigma_{\psi b}$ (MPa)	0.323
θ_{HTT} (MPa °C h)	220.0	θ_{HaloTT} (M °C h)	74.9	θ_{HTT} (MPa °C h)	320.0
k_T (MPa °C^{-1})	0.066	k_T (M °C^{-1})	0.024	k_T (MPa °C^{-1})	0.10
T_d (°C)	30.0	T_d (°C)	30.0	T_d (°C)	30.0
Cardinal Ts at 0 MPa		Cardinal Ts at 0 M		Cardinal Ts at 0 MPa	
T_b (°C)	4.80	T_b (°C)	4.80	T_b (°C)	4.80
T_o (°C)	30.0	T_o (°C)	30.0	T_o (°C)	30.0
T_c (°C)	43.0	T_c (°C)	43.0	T_c (°C)	43.0
R^2	0.86	R^2	0.83	R^2	0.83

T_c calculated by extrapolation from the germination rate data at Ts above T_o. R^2 is the coefficient of determination

The T_d was equal to T_o in the present study

salt and control treatments, but with less decrease for salt treatments. SMC tended to increase with NaCl at each T, but decreased as T increased to T_o then increased again. The reason for the decrease in SMC with increasing T is unclear, but may be due to more rapid GR_{50} around T_o and less time to achieve maximum moisture content prior to radicle emergence. At $Ts \geq 35$ °C, the SMC increased and tended to increase with increasing NaCl concentrations relative to control (Fig. 6a).

At all Ts, Na^+ concentration in the seed tissues increased significantly with increasing NaCl ($p < 0.05$) when compared to the control, attaining 132 mmol kg^{-1} DW at 0.300 M NaCl (Fig. 6b). Cl^- content of chicory seeds also increased remarkably as salinity levels increased ($p < 0.05$) at all Ts (Fig. 6c). Seed Cl^- content reached its highest levels at supra-optimal Ts (> 30 °C) (Fig. 6c).

As the median base water potentials preventing germination were −0.5 MPa lower in NaCl in comparison with PEG (Table 2; Fig. 3b), we estimated the osmotic adjustment in the seeds that could be attributed to additional Na^+ and Cl^- ion uptake. Using the ion contents and water contents on a dry weight basis, we calculated the total NaCl concentrations in the seeds for each treatment and converted these into osmotic potential values. These values were approximately −0.5 MPa in water and became more negative as NaCl concentration increased, reaching approximately −1.3 MPa across Ts at 0.300 M (Fig. 6d). Thus, sufficient Na^+ and Cl^- ions were taken up by the seeds to account for the observed ability of seeds to germinate to lower osmotic potential in salt as compared to PEG, which does not enter the cells. Osmotic adjustment due to NaCl uptake is also consistent with the increase in SMC with increasing NaCl concentration (Fig. 6a), while SMC decreases with increasing PEG concentration (Bradford

1986). There is uncertainty as to the locations of the ions and the water inside of the seed tissues (i.e., apoplastic or symplastic), and only symplastic ions would presumably contribute to increasing turgor and therefore to germination capacity. Nonetheless, the data indicate that salt ion uptake into the seeds was at least sufficient to account for the differences between $\psi_b(50)$ and $NaCl_b(50)$ (converted to osmotic potential) (Table 3; Fig. 3b).

Discussion

In general, the temperature responses of seeds can be defined by their cardinal Ts (i.e., T_b, T_o and T_c) (Bewley et al. 2013). The relationship between GR_{50} and T identified values of 4.8, 30 and 43 °C for T_b, T_o and T_c, respectively (Table 3). Similar T_b values have been reported for witloof chicory (*Cichorium intybus*; 5.3 °C) (Bierhuizen and Wagenvoort 1974), chicory (*Cichorium intybus* cv. Grasslands Puna; 3.7 °C) (Moot et al. 2000) and rapeseed (0–5 °C, depending on cultivars) (Farzaneh et al. 2014). The maximum GR_{50} was observed at 30 °C (T_o) in the control treatment (0 MPa and 0 M), similar to previous reports for chicory (29.9 °C, Zarghani et al. 2014; 25 to 30 °C, Corbineau and Come 1989), although Balandary et al. (2011) reported a value of 25.5 °C after fitting an empirical beta model. Our findings showed also that T_b and T_o were relatively unaffected by PEG and NaCl stresses, which corroborate results for T_o of *Silybum marianum* and *Calendula officinalis* (Parmoon et al. 2018) and flax-leaf alyssum (*Alyssum linifolium* Steph. ex. Willd.) (Mobli et al. 2018). The median T_c value estimated in this study (43 °C based on both hydrotime and
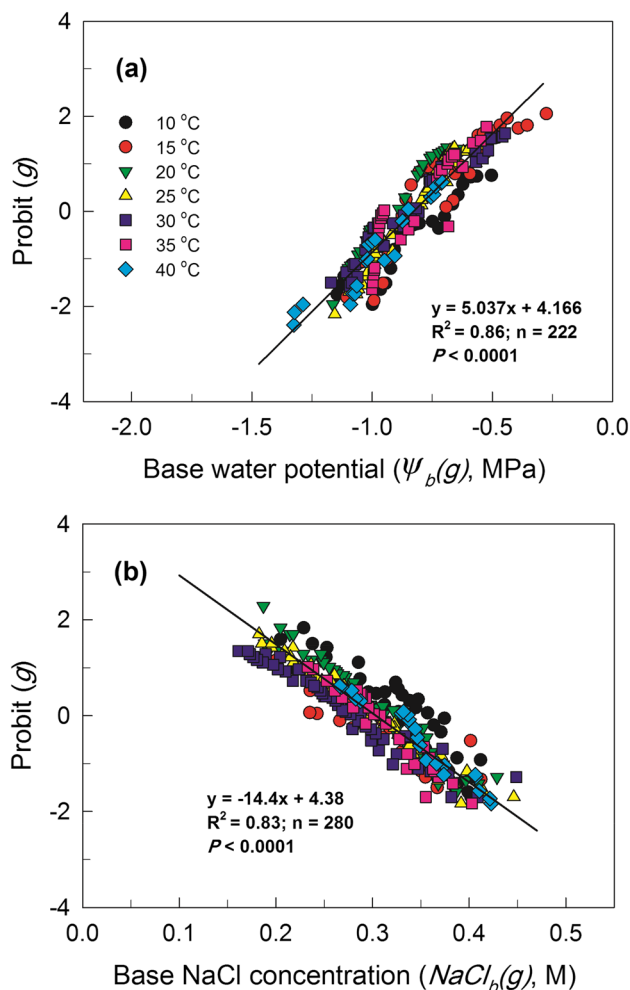
Fig. 5 Linear regression of probit (g) plotted against base water potentials ($\psi_b(g)$, MPa) and adjusted base water potentials ($\psi_b(g) + k_T(T - T_d)$) (**a**) and linear regression of probit (g) plotted against base NaCl concentrations (NaCl$_b$(g), M) and adjusted base NaCl concentrations ($-NaCl_b(g) + k_T(T - T_d)$) (**b**). Symbols are the observed values of probit germination fraction at each T versus the calculated base values for different germination fractions (g). The highly significant linear relationships with probit (g) indicate that the base thresholds are normally distributed in the seed population and that the hydrothermal and halothermal models account for 83–86% of the variance in the germination behavior across all conditions

halotime models) was approximately equal to the values reported for chicory by Zarghani et al. (2014) (46.3 °C) and Vahabinia et al. (2019) (40.2 °C) based on different models. At $T > T_o$, the value of T_c varies among seeds in the population (Alvarado and Bradford 2002), and also depends upon the stress level (Atashi et al. 2014; Bakhshandeh et al. 2017; Parmoon et al. 2018; Abdellaoui et al. 2019). As stress intensity increases, T_c approaches nearer to T_o, as illustrated here for chicory (Fig. 4), because of the threshold sensitivities to ψ or NaCl increase as the T increases above T_o (Fig. 3c, d).

The HTT model (Gummerson 1986), generalized as population-based threshold models, describes well the observed GRs and GPs response to increasing stress, aging, hormones and other factors affecting seed germination (Bello and Bradford 2016). GR$_{50}$ slows as the stress intensity increases due to reduced ψ or increased NaCl concentrations, and GP also declines as the stress exceeds the threshold that prevents germination for a given fraction of the seed population. The HTT and HaloTT models applied here described these patterns well for chicory seeds (Figs. 1, 2, 5). The time constants in these models (e.g., θ_H or θ_{Halo}) provided useful overall values for germination kinetics for estimating the cardinal Ts under both water and salt stress (Fig. 3). Following the work of Seal et al. (2018) on the halophyte *Suaeda maritima*, we used the NaCl concentrations to fit halotime and HaloTT models to our germination data for chicory seeds. In the suboptimal T range, NaCl$_b$(50) was not affected by NaCl concentration (Fig. 3d), which is in contrast to the results reported by Seal et al. (2018), who found that NaCl$_b$(50) values significantly decreased with increasing T (between 5 and 25 °C). In contrast, threshold values in the halophyte *Chloris virgata* and the glycophyte *Digitaria sanguinalis* tended to increase with T before declining (Zhang et al. 2012). Thus, these responses may vary among species and the environments to which they are adapted (Huarte 2006). In addition, we extended the HaloTT model for quantifying SG responses at $Ts > T_o$. The NaCl$_b$(50) values for chicory decreased linearly above T_o, consistent with seed germination responses to ψ at high temperature (Alvarado and Bradford 2002). Thus, germination patterns across the entire range of temperatures from T_b to T_c could be described by the HaloTT model on the basis of NaCl concentration (Figs. 4a, d; 5b).

However, SG characteristics of chicory were more influenced by ψ in comparison with NaCl at equivalent osmotic potentials (Table 2). This agrees with the findings for other species, such as soybean (Khajeh-Hosseini et al. 2003), alfalfa (Tilaki et al. 2009), barley (Zhang et al. 2010), sunflower (Luan et al. 2014) and rapeseed (Bakhshandeh and Jamali 2020). This is likely due to the uptake of salt ions by the chicory seed, enabling osmotic adjustment to maintain a ψ gradient allowing water uptake during imbibition and germination (Heshmat et al. 2011; Seal et al. 2018). SMC, Na$^+$ and Cl$^-$ concentrations increased in chicory seeds with increasing salinity (Fig. 6), consistent with results with barley (Zhang et al. 2010), several halophytic species (Khan et al. 1985; Seal et al. 2018; Song et al. 2005) and rapeseed (Bakhshandeh and Jamali 2020). In our case, the measured uptake of Na$^+$ and Cl$^-$ ions during imbibition in salt solutions was sufficient to account for the lower apparent $\psi_b(50)$ values when NaCl was converted to osmotic potentials. As the halotime model described germination behavior well up to the highest NaCl tested (0.300 M), chicory SG is controlled primarily by the osmotic rather than toxic effects of
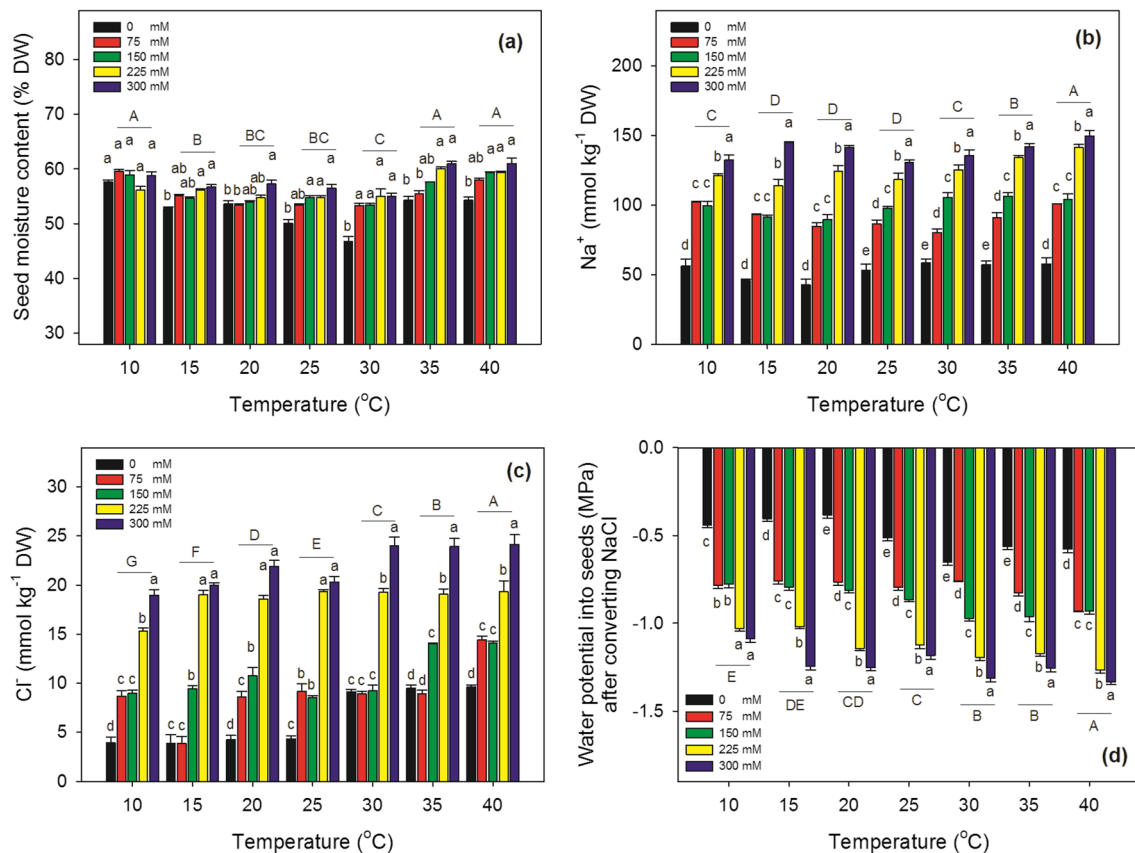
Fig. 6 Seed moisture content (**a**), concentrations of Na$^+$ (**b**), Cl$^-$ (**c**) and calculated osmotic potential due to NaCl (**d**) into the chicory seeds. Lower case letters show significant differences among NaCl treatments within a temperature and upper case letters show significant differences among temperatures, using the least significant difference test (LSD) at 0.05 probability level

salt, as also reported for barley (Zhang et al. 2010), *Acacia harpophylla* (Arnold et al. 2014) and *Atriplex halimus* (Shaygan et al. 2017).

In conclusion, the models used in this work accurately and successfully describe chicory SG across all *Ts* at a range of *ψ*s and NaCls and provide reliable tools for assessing germination under these conditions. We developed a HaloTT model for quantifying the SG responses (both GR and GP) in the supra-optimal *T* range, which has not been reported previously. This model was also able to predict germination responses of salt tolerant (rapeseed), moderately salt-sensitive (cucumber), and salt-sensitive (green bean) species (Bakhshandeh et al. unpublished data). Thus, the hydrotime, halotime, HTT and HaloTT models enable prediction of SG behavior across entire the range of temperature, water and salt conditions.

Of course, conditions can vary in the field and performance may not exactly match model predictions. However, we note that Liu et al. (2020) used the HTT model to characterize germination behavior of 13 native desert annual species. They found that relative germination sensitivities to *T* and *ψ* determined from laboratory tests were highly correlated with average seedling emergence data in desert conditions over 25 years of field observations in Arizona. Both HTT and HaloTT models use parameters based on mechanistic assumptions about the underlying physiology of SG to describe patterns of germination timing. Therefore, we believe that while field conditions can vary and influence germination at a particular time, the HaloTT model developed here can quantify and predict the relative germination performance that can be expected in field conditions.

Author contribution statement EB and KB designed the experiments. EB and FV performed the experiments. EB and KB conducted the modeling and interpreted the data. EB, KB, HP, FV and RA co-wrote all drafts of the paper and also approved the final draft for submission.

Compliance with ethical standards

Conflict of interest The authors declare no conflicts of interest.

References

Abbas ZK, Saggu S, Sakeran MI, Zidan N, Rehman H, Ansari AA (2015) Phytochemical, antioxidant and mineral composition of hydroalcoholic extract of chicory (*Cichorium intybus* L.) leaves. Saudi J Biol. Sci. 22:322–326

Abdellaoui R, Boughalleb F, Zayoud D, Neffati M, Bakhshandeh E (2019) Quantification of *Retama raetam* seed germination response to temperature and water potential using hydrothermal time concept. Environ Exp Bot 157:211–216

Alvarado V, Bradford K (2002) A hydrothermal time model explains the cardinal temperatures for seed germination. Plant Cell Environ 25:1061–1069

Arnold S, Kailichova Y, Baumgartl T (2014) Germination of Acacia harpophylla (Brigalow) seeds in relation to soil water potential: implications for rehabilitation of a threatened ecosystem. PeerJ 2:e268

Atashi S, Bakhshandeh E, Zeinali Z, Yassari E, Teixeira da Silva JA (2014) Modeling seed germination in *Melisa officinalis* L. in response to temperature and water potential. Acta Physiol Plant 36:605–611

Atashi S, Bakhshandeh E, Mehdipour M, Jamali M, Teixeira da Silva JA (2015) Application of a hydrothermal time seed germination model using the Weibull distribution to describe base water potential in zucchini (*Cucurbita pepo* L.). J Plant Growth Regul 34:150–157

Bakhshandeh E, Gholamhossieni M (2018) Quantification of soybean seed germination response to seed deterioration under PEG-induced water stress using hydrotime concept. Acta Physiol Plant 40:126

Bakhshandeh E, Gholamhossieni M (2019) Modelling the effects of water stress and temperature on seed germination of radish and cantaloupe. J Plant Growth Regul. https://doi.org/10.1007/s00344-00019-09942-00349

Bakhshandeh E, Jamali M (2020) Population-based threshold models: a reliable tool for describing aged seeds response of rapeseed under salinity and water stress. Environ Exp Bot. https://doi.org/10.1016/j.envexpbot.2020.104077

Bakhshandeh E, Atashi S, Hafez-Nia M, Pirdashti H (2013) Quantification of the response of germination rate to temperature in sesame (*Sesamum indicum*). Seed Sci Technol 41:469–473

Bakhshandeh E, Atashi S, Hafeznia M, Pirdashti H, Teixeira da Silva JA (2015) Hydrothermal time analysis of watermelon (*Citrullus vulgaris* cv 'Crimson sweet') seed germination. Acta Physiol Plant 37:1738

Bakhshandeh E, Jamali M, Afshoon E, Gholamhossieni M (2017) Using hydrothermal time concept to describe sesame (*Sesamum indicum* L.) seed germination response to temperature and water potential. Acta Physiol Plant 39:250

Bakhshandeh E, Pirdashti H, Vahabinia F, Gholamhossieni M (2019) Quantification of the effect of environmental factors on seed germination and seedling growth of Eruca (*Eruca sativa*) using mathematical models. J Plant Growth Regul. https://doi.org/10.1007/s00344-00019-09974-00341

Bakhshandeh E, Gholamhosseini M, Yaghoubian Y, Pirdashti H (2020) Plant growth promoting microorganisms can improve germination, seedling growth and potassium uptake of soybean under drought and salt stress. Plant Growth Regul 90:123–136

Balandary A, Rezvani Moghaddam P, Nasiri Mahalati M (2011) Determination of seed germination cardinal temperatures in short chicory (*Cichorium pumilum* Jacq.). Second National Seed Technology Conference, Mashhad, pp 1818–1822

Baskin CC, Baskin JM (2014) Seeds: ecology, biogeography, and evolution of dormancy and germination. Academic, San Diego, p 1600

Bello P, Bradford KJ (2016) Single-seed oxygen consumption measurements and population-based threshold models link respiration and germination rates under diverse conditions. Seed Sci Res 26:199–221

Benítez G, González-Tejero M, Molero-Mesa J (2010) Pharmaceutical ethnobotany in the western part of Granada province (southern Spain): ethnopharmacological synthesis. J Ethnopharmacol 129:87–105

Bewley JD, Bradford K, Hilhorst H, Nonogaki H (2013) Seeds: physiology of development, germination and dormancy, 3rd edn. Springer, New York

Bierhuizen J, Wagenvoort W (1974) Some aspects of seed germination in vegetables. 1. The determination and application of heat sums and minimum temperature for germination. Sci Hortic 2:213–219

Bradford KJ (1986) Manipulation of seed water relations via osmotic priming to improve germination under stress conditions. HortScience 21:1105–1112

Bradford KJ (1990) A water relations analysis of seed germination rates. Plant Physiol 94:840–849

Bradford KJ (1995) Water relations in seed germination. Seed Dev Germ 1:351–396

Bradford KJ (2002) Applications of hydrothermal time to quantifying and modeling seed germination and dormancy. Weed Sci 50:248–260

Bradford KJ, Still DW (2004) Applications of hydrotime analysis in seed testing. Seed Technol 26:75–85

Corbineau F, Come D (1989) Germinability and quality of *Cichorium intybus* L. seeds. VI Symp Timing Field Prod Veg 267:183–190

Dahal P, Bradford KJ (1994) Hydrothermal time analysis of tomato seed germination at suboptimal temperature and reduced water potential. Seed Sci Res 4:71–80

Estefan G, Sommer R, Ryan J (2013) Methods of soil, plant, and water analysis. A manual for the West Asia and North Africa region, International Center for Agricultural Research in the Dry Areas (ICARDA), p 244

Farzaneh S, Soltani E, Zeinali E, Ghaderi-Far F (2014) Screening oilseed rape germination for thermotolerance using a laboratory-based method. Seed Technol 15–27

Ghaderi-Far F, Bakhshandeh E, Ghadirian R (2010) Evaluating seed quality in sesame (*Sesamum indicum* L.) by the accelerated ageing test. Seed Technol 32:69–72

Guarrera P, Savo V (2016) Wild food plants used in traditional vegetable mixtures in Italy. J Ethnopharmacol 185:202–234

Gummerson R (1986) The effect of constant temperatures and osmotic potentials on the germination of sugar beet. J Exp Bot 37:729–741

Hatfield JL, Prueger JH (2015) Temperature extremes: effect on plant growth and development. Weather Clim Extrem 10:4–10

Heshmat O, Saeed H, Fardin K (2011) The improvement of seed germination traits in canola (*Brassica napus* L.) as affected by saline and drought stress. J Agric Sci Technol 7:611–622

Huarte R (2006) Hydrotime analysis of the effect of fluctuating temperatures on seed germination in several non-cultivated species. Seed Sci Technol 34:533–547

International Seed Testing Association (ISTA) (2018) International rules for seed testing. Seed Science and Technology, Zurich

Jouad H, Haloui M, Rhiouani H, El Hilaly J, Eddouks M (2001) Ethnobotanical survey of medicinal plants used for the treatment of

diabetes, cardiac and renal diseases in the North centre region of Morocco (Fez–Boulemane). J Ethnopharmacol 77:175–182

Kamkar B, Al-Alahmadi MJ, Mahdavi-Damghani A, Villalobos FJ (2012) Quantification of the cardinal temperatures and thermal time requirement of opium poppy (*Papaver somniferum* L.) seeds to germinate using non-linear regression models. Ind Crops Prod 35:192–198

Khajeh-Hosseini M, Powell A, Bingham I (2003) The interaction between salinity stress and seed vigour during germination of soyabean seeds. Seed Sci Technol 31:715–725

Khan M, Weber D, Hess W (1985) Elemental distribution in seeds of the halophytes Salicornia pacifica var. utahensis and Atriplex canescens. Am J Bot 72:1672–1675

Liu S, Bradford KJ, Huang Z, Venable DL (2020) Hydrothermal sensitivities of seed populations underlie fluctuations of dormancy states in an annual plant community. Ecology 101(3):e02958

Llanes A, Andrade A, Masciarelli O, Alemano S, Luna V (2016) Drought and salinity alter endogenous hormonal profiles at the seed germination phase. Seed Sci Res 26:1–13

Luan Z, Xiao M, Zhou D, Zhang H, Tian Y, Wu Y, Guan B, Song Y (2014) Effects of salinity, temperature, and polyethylene glycol on the seed germination of sunflower (*Helianthus annuus* L.). Sci World J 2014:170418. https://doi.org/10.1155/2014/170418

Mesgaran M, Mashhadi H, Alizadeh H, Hunt J, Young K, Cousens R (2013) Importance of distribution function selection for hydrothermal time models of seed germination. Weed Res 53:89–101

Mesgaran MB, Onofri A, Mashhadi HR, Cousens RD (2017) Water availability shifts the optimal temperatures for seed germination: a modelling approach. Ecol Model 351:87–95

Michel BE, Radcliffe D (1995) A computer program relating solute potential to solution composition for five solutes. Agron J 87:126–130

Mobli A, Ghanbari A, Rastgoo M (2018) Determination of cardinal temperatures of Flax-leaf Alyssum (*Alyssum linifolium*) in response to salinity, pH, and drought stress. Weed Sci 66:470–476

Moltchanova E, Sharifiamina S, Moot DJ, Shayanfar A, Bloomberg M (2020) Comparison of three different statistical approaches (non-linear least-squares regression, survival analysis and Bayesian inference) in their usefulness for estimating hydrothermal time models of seed germination. Seed Sci Res. https://doi.org/10.1017/S0960258520000082

Moot D, Scott W, Roy A, Nicholls A (2000) Base temperature and thermal time requirements for germination and emergence of temperate pasture species. New Zealand J Agric Res 43:15–25

Nobel PS (1983) Biophysical plant physiology and ecology. W. H. Freeman and Co., San Francisco

Parihar P, Singh S, Singh R, Singh VP, Prasad SM (2015) Effect of salinity stress on plants and its tolerance strategies: a review. Environ Sci Pollut Res 22:4056–4075

Parmoon G, Moosavi SA, Siadat SA (2018) How salinity stress influences the thermal time requirements of seed germination in *Silybum marianum* and *Calendula officinalis*. Acta Physiol Plant 40:175

Rowse H, Finch-Savage W (2003) Hydrothermal threshold models can describe the germination response of carrot (Daucus carota) and onion (Allium cepa) seed populations across both sub-and supra-optimal temperatures. New Phytol 158:101–108

Sampaio FC, Maria do Socorro VP, Dias CS, Costa VCO, Conde NC, Buzalaf MA (2009) In vitro antimicrobial activity of *Caesalpinia ferrea* Martius fruits against oral pathogens. J Ethnopharmacol 124:289–294

SAS Institute Inc (2015) SAS/STAT user's guide. SAS Institute Inc., Cary

Seal CE, Barwell LJ, Flowers TJ, Wade EM, Pritchard HW (2018) Seed germination niche of the halophyte Suaeda maritima to combined salinity and temperature is characterised by a halothermal time model. Environ Exp Bot 155:177–184

Shaygan M, Baumgartl T, Arnold S (2017) Germination of Atriplex halimus seeds under salinity and water stress. Ecol Eng 102:636–640

Song J, Feng G, Tian C, Zhang F (2005) Strategies for adaptation of Suaeda physophora, Haloxylon ammodendron and Haloxylon persicum to a saline environment during seed-germination stage. Ann Bot 96:399–405

Tilaki GAD, Behtari B, Behtari B (2009) Effect of salt and water stress on the germination of alfalfa (*Medicago sativa* L.) seed. Поволжский экологический журнал, 158–164

Vahabinia F, Pirdashti H, Bakhshandeh E (2019) Environmental factors' effect on seed germination and seedling growth of chicory (*Cichorium intybus* L.) as an important medicinal plant. Acta Physiol Plant 41:27

Van't Hoff JH (1887) The role of osmotic pressure in the analogy between solutions and gases. Zeitschrift fur physikalische Chemie 1:481–508

Wang R, Bai Y, Tanino K (2005) Germination of winterfat (*Eurotia lanata* (Pursh) Moq.) seeds at reduced water potentials: testing assumptions of hydrothermal time model. Environ Exp Bot 53:49–63

Yoo S, Murata R, Duarte S (2011) Antimicrobial traits of tea-and cranberry-derived polyphenols against Streptococcus mutans. Caries Res 45:327–335

Zarghani H, Mijani S, Nasrabadi SE (2014) Temperature effects on the seed germination of some perennial and annual species of Asteraceae family. Plant Breed Seed Sci 69:3–14

Zhang H, Irving LJ, McGill C, Matthew C, Zhou D, Kemp P (2010) The effects of salinity and osmotic stress on barley germination rate: sodium as an osmotic regulator. Ann Bot 106:1027–1035

Zhang H, Irving L, Tian Y, Zhou D (2012) Influence of salinity and temperature on seed germination rate and the hydrotime model parameters for the halophyte, Chloris virgata, and the glycophyte, Digitaria sanguinalis. South Afr J Bot 78:203–210